

Characterizing Fiber Nonlinearity with Deployed Equipment in Optical Line Systems

Yinqing Pei, Alex W. MacKay*, Mehrnoosh Boroojerdi, Jean-Luc Archambault, David W. Boertjes

Ciena Corporation, 383 Terry Fox Dr., Ottawa, Ontario, Canada, K2K 0L1

Author e-mail address: amackay@ciena.com

Abstract: We introduce the first measurement procedure to characterize fiber nonlinear parameters of all fibers in an optical network using widely deployed network equipment which does not rely on modem measurements or external instrumentation. © 2024 The Author(s)

1. Introduction

Understanding fiber nonlinear characteristics is essential for accurate quality of transmission (QoT) modeling and SNR optimization of optical networks. For each span, the loss coefficient, α , the propagation coefficient, β , and the nonlinear coefficient, γ , are needed, along with fiber length and power spectral density (PSD) at fiber input to accurately model nonlinear QoT [1,2]. Fiber length and α can be extracted from OTDR traces, and PSD can be obtained from optical channel monitors (OCMs), which are mid-resolution optical spectrum analyzers (OSAs), all of which are commonly deployed in modern photonic network equipment. However, obtaining γ and β remains more challenging. There are fiber type detection methods [3] to alleviate this, but the variations of characteristics of fiber within a fiber “type” may make this insufficient. Also, after a fiber is deployed into a network, there are new patch panel losses (PPLs) and other losses that change the equivalent fiber characteristics. Finally, heterogeneous spans comprised of multiple segments of different fibers will have nonlinear characteristics which do not match any pre-defined fiber “type”.

In this paper, we introduce a fiber nonlinear characterization method which does not rely on high performance modems or any sophisticated measurement apparatus. The technique allows determination of equivalent fiber nonlinear parameters which remove uncertainty in QoT modeling and optimization when utilized in common nonlinear modeling techniques [1,2].

2. Equivalent fiber model

To simplify system modeling, we propose the concept of an equivalent fiber model, analogous to an equivalent circuit model in electronics. The purpose is to generate the coefficients of a uniform equivalent fiber which produces similar nonlinear interference (NLI) as the actual span. The parameters of interest are an equivalent nonlinear coefficient, γ_{eq} , and an equivalent dispersion as a function of frequency $D_{eq}(\nu)$, which corresponds to the equivalent group-velocity dispersion parameter, $\beta_{2,eq}(\nu) = -\frac{c}{2\pi\nu^2} D_{eq}(\nu)$, where c is the speed of light.

3. Measurement overview

The fiber characterization consists of two sets of measurements across each optical multiplex section (OMS), between two reconfigurable optical add-drop multiplexers (ROADMs).

3.1. SRS measurement for γ_{eq}

There is no known method of measuring γ without requiring narrow band sources and high-resolution OSAs [4] or coherent receivers [5]. However, these measurements are not cost effective in large optical networks. We propose a simple method of backing out γ of an equivalent fiber span based on measurement of stimulated Raman scattering (SRS). Since both γ and the Raman gain efficiency, C_R , are inversely proportional to fiber effective area [6,7], the following equality approximately holds in typical transmission fibers $\gamma_{eq}/\gamma_{ref} \approx C_{R,eq}/C_{R,ref}$, so that we can determine the γ_{eq} directly if we can measure an $C_{R,eq}/C_{R,ref}$ and utilize a known reference fiber, such as NDSF, for γ_{ref} and $C_{R,ref}$.

To measure $C_{R,eq}/C_{R,ref}$, we utilize the out-of-band optical supervisory channel (OSC) as a probe which terminates between line-amp sites, and use an amplified spontaneous emission (ASE) source as a co-propagating pump. In our measurement, we fix the OSC transmit power on each span and switch the ASE power between an on and off state. We launch the ASE power in the on state much higher than the OSC to ensure we are operating in the non-depleted regime [6]. We measure the on-off gain at the OSC frequency in dB units by the difference in received

OSC power between the state with and without ASE pumping, ΔOSC , where $\Delta\text{OSC} = \frac{10}{\ln 10} C_R \frac{1 - \exp(-\alpha L)}{\alpha} P_{\text{ASE}, \text{Tx}, \text{ON}}$, C_R is the Raman gain efficiency between the OSC frequency and ASE pump, L is the fiber length, α is the fiber loss coefficient and $P_{\text{ASE}, \text{Tx}, \text{ON}}$ is the launch power of the ASE in on state in linear units [6]. The measured ΔOSC will be compared with a reference $\Delta\text{OSC}_{\text{ref}(L, \alpha)}$ on a simulated, known fiber with the same L , α , and $P_{\text{ASE}, \text{Tx}, \text{ON}}$, so we can isolate the ratio of Raman gain efficiencies, therefore:

$$\gamma_{eq} \approx \frac{\Delta\text{OSC}}{\Delta\text{OSC}_{\text{ref}(L, \alpha)}} \cdot \gamma_{\text{ref}}. \quad (1)$$

To get the best resolution from the measurement, we filter the ASE source such that it has a large frequency separation from the OSC to maximize the Raman gain efficiency as shown in Fig. 1(a). Fig.1(b) shows a pre-computed reference trace based on NDSF fiber type at $\alpha = 0.2$ dB/km.

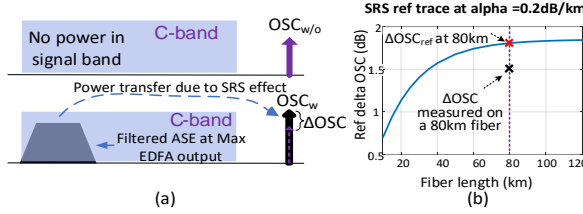


Fig. 1 (a) Illustration of the SRS measurement. (b) an example reference trace of the SRS measurement.

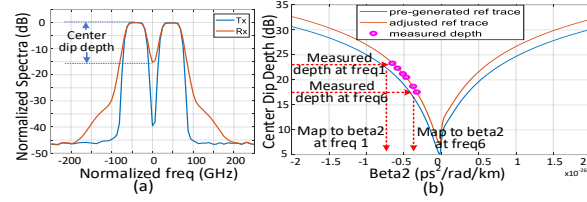


Fig. 2 (a) Illustration of the broadening effect. (b) fitting measured depth to reference trace in DPS measurement.

3.2. Spectral broadening measurement for D_{eq}

The second measurement utilizes Kerr-induced spectral broadening, observed at very high launch powers, to back out $D_{eq}(\nu)$. A shaped ASE dual-peak spectrum (DPS) is created using the built-in ASE source and wavelength selective switch (WSS) at the Transmit (Tx) ROADM into the OMS. The amplifiers in the section are configured to generate very high launch power into one span at a time and low power into the other spans to excite NLI, and therefore observe broadening, primarily in the span under test (SUT). The broadened spectrum is measured with the OCM on the Receive (Rx) ROADM. Fig. 2(a) shows a comparison between the DPS at the Tx and Rx side. The broadening effect at the Rx side is characterized by the ratio between peak and valley of the DPS, denoted as center dip depth (CDD). The DPS is set to different frequencies to measure dispersion across the signal band. The CDD as a function of frequency is compared with a set of pre-generated reference traces to back out the $D_{eq}(\nu)$, and $\beta_2(\nu)$ of the SUT. As shown in Fig. 2(b), a sample pre-computed reference trace of the CDD as a function of β_2 is selected for the length, launch power, and α of the SUT. The vertical axis of the reference trace is adjusted based on γ_{eq} from the SRS measurement and the launch power at the output of the amplifier into the SUT. The depths measured at different frequencies will be fitted to the depths of the adjusted reference trace to get the equivalent dispersion at different frequencies.

4. Experiment and results

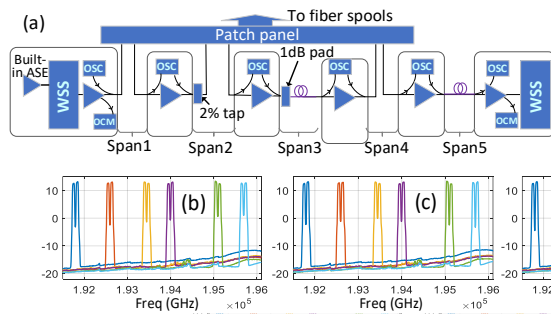


Fig. 3 (a) Experimental setup, (b)~(f) Rx DPS at the six measured frequencies of each span.

Table 1. Fiber data in the system

	span1	span2	span3	span4	span5
	5km TWC→15km eLEAF→45km NDSF	60km DSF	1dB pad → 80km eLEAF	120km NDSF	80km eLEAF
γ_{eq} (/W/km)	0.86	0.93	1.02	0.79	1.29
$P_{\text{SUT}}(\text{dBm})$	17	14.2	18.6	22.3	18.1

The measurement is run on a 5-span OMS using Ciena Reconfigurable Line System hardware as shown in Fig. 3 (a). Fibers used in each span are listed in Table. 1. Fibers in spans 1, 2 and 4 are connected to the system through a patch panel, while the fibers in spans 3 and 5 are not, to better control the loss between the amplifier and the fiber for the γ_{eq} demonstration in the next section.

First, the SRS measurement is performed. The launch power of the pump in the on state is 23 dBm. The backed out γ_{eq} are shown in Table. 1. The spectral broadening measurement is performed next. For each SUT, we adjust the

launch power at each SUT such that the DPS is operating in the NLI dominant regime to achieve a CDD with good sensitivity to read off from the Rx OCM spectrum, but before the regime where we have a discontinuity in the reference curve. To do this, we target a measured CDD of around 10 to 20 dB observed from Fig. 2(b). The launch powers of each SUT in the spectral broadening measurement are listed in Table.1, and the spans not under test have launch power 10 dB lower than SUT. At each SUT, the DPS is swept at six frequencies. The Rx DPS is measured with an OCM with a 12.5 GHz resolution bandwidth. The subplots in Fig. 3 (b)-(f) show the overlaid Rx DPS when measuring one SUT. The equivalent dispersion is then backed out from center dip depth after removing modeled linear noise using the tools described in [8]. Fig. 4 shows the measured equivalent dispersion versus dispersion of each fiber measured by a Viavi T-BERD 8000.

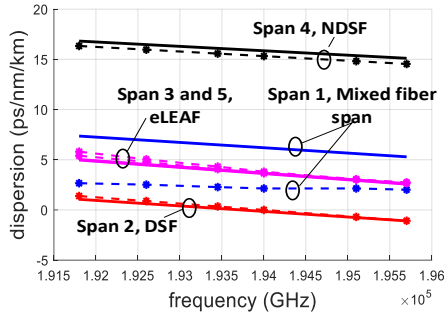


Fig. 4 Measured eqv. dispersion (dashed star lines) VS bench top instrument measured linear dispersion (solid lines)

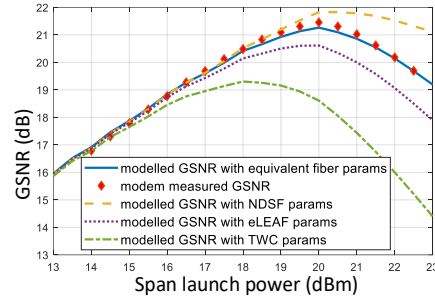


Fig.5 GSNR of span 1, measured VS modeled.

5. Equivalent parameter discussion

As shown in Table.1, the measured γ_{eq} of each span differs from the expected γ of the corresponding fiber type as γ_{eq} includes the impact of PPL. A 1 dB PPL results in 1 dB lower γ_{eq} . This is demonstrated by the γ_{eq} results of the two 80 km eLEAF spans, i.e. span 3 and 5, where a 1 dB attenuator is placed before the fiber input of span 3. The difference of γ_{eq} of span 3 and 5 reflects the 1dB difference in PPL, where $10 \cdot \log_{10}(1.29/1.02) = 1.02 \approx 1 \text{ dB}$.

Fig.4 shows the $D_{eq}(\nu)$ matches well with the reference dispersion in spans with a single fiber type to better than 0.8 ps/nm/km across all frequencies and homogeneous fibers. The equivalent dispersion of span 1 does not match the bench-top instrument measured dispersion because it is a heterogeneous span and the dispersion measured by the Viavi T-BERD 8000 is the linear dispersion based on group delay. However, the dispersion of the fiber near the beginning of the span contributes more to the NLI experienced in the span which is captured by the equivalent dispersion.

To validate the utility of the measured equivalent fiber nonlinear parameters, we compare the modeled generalized signal-to-noise ratio (GSNR) using the equivalent parameters through a standard GN model [1] to direct modem measurements on a heterogeneous fiber span (span 1). We varied the launch power of a 62.5 Gbaud, 400 Gb/s coherent modem over span 1 and monitored the received SNR. Fig.5 plots the coherent modem measured GSNR versus the modeled GSNR. The NLI was modeled using the equivalent nonlinear parameters of span 1 as well as quoted nonlinear parameters of NDSF, eLEAF and TWC for comparison. As shown in Fig. 5, the modeled GSNR curve based on the proposed equivalent nonlinear parameters matches well with the modem measured GSNR to within 0.2 dB at all points and was able to determine the optimal launch power. In contrast, the modeled curves based on any single fiber type not only diverged from the modem measured GSNR in the nonlinear region, but also incorrectly predict optimal launch power and GSNR, which will result in compromised performance optimization and inaccurate link budgeting.

6. Conclusion

We have proposed and demonstrated a measurement procedure for equivalent fiber nonlinear parameters using deployed equipment in optical line systems. The measurement accuracy of equivalent dispersion across frequency is better than 0.8 ps/nm/km and GSNR can be predicted to within 0.2 dB accuracy across launch power on a heterogeneous span.

7. References

- [1]. P. Poggiolini et al., *Photonics technology letters* 23(11), 742(2011).
- [2]. O. V. Sinkin, et al., *J. Lightwave Technol.*, 21(1), 61(2003).
- [3]. E. Seve, et al., *J. Lightwave Technol.*, 37(7), 1724(2019).
- [4]. Y. Namiyama, et al., *NIST Special Publication*, 988,15(2002).
- [5]. L. S. Schanner, et al., *IMOC*, 1(2021).
- [6]. J. Bromage, et al., *J. Lightwave Technol.*, 22(1), 79(2004).
- [7]. G P. Agrawal, *Nonlinear Fiber Optics*, 2nd edition, Chapter 2, 28(1995).
- [8]. A. W. MacKay, et al., *OFC '2022*, W4G.2(2022).